Dalton Trans.

ARTICLE

Self-Assembly of heteroleptic dinuclear silver(I) complexes bridged by bis(diphenylphosphino)ethyne

Cite this: DOI: 10.1039/x0xx00000x

Sarah Keller,[a] Timothy N. Camenzind,[a,b] Johannes Abraham,[c] Alessandro Prescimone,[a] Daniel Häussinger,[c] Edwin C. Constable[a] and Catherine E. Housecroft*[a]

Received 00th January 2012,
Accepted 00th January 2012

DOI: 10.1039/x0xx00000x

www.rsc.org/

We present a study of the self-assembling behaviour in solution of $Ag[PF_6]$ with one equivalent of an N^N ligand (N^N = 6,6'-dimethyl-2,2'-bipyridine (6,6'-Me_2bpy) or 2,2':6',2''-terpyridine (tpy)), together with either 0.5 or one equivalent of the bridging ligand bis(diphenylphosphino)ethyne (dppa). Each product contains a dinuclear cation, with one or two dppa ligands bridging the two Ag^+ centres; 6,6'-Me_2bpy and tpy, respectively, act as chelating ligands. The compounds have been analysed in solution using NMR spectroscopic methods (^{1}H, ^{1}H{^{31}P}, COSY, NOESY, ^{13}C, HMQC and HMBC), including room and low temperature measurements. ^{31}P{^{1}H} NMR spectra recorded at different temperatures allow a deeper insight into the dynamic equilibrium processes. In addition, solution ^{31}P-^{109}Ag HSQC spectroscopic measurements were performed and show, *inter alia*, the ratio of the splitting in the F1 dimension and the $^1J_{31P\text{-}109Ag}$ coupling constant in the fully coupled HSQC. Single crystal X-ray diffraction yielded two pseudo-polymorphic structures for the doubly-bridged $[Ag_2(dppa)_2(tpy)_2][PF_6]_2$ and one for the singly-bridged $[Ag_2(dppa)(6,6'\text{-}Me_2bpy)_2][PF_6]_2$.

Introduction

Copper(I) complexes are emerging from fundamental research into applications such as dye-sensitized solar cells and light-emitting devices[1,2]. For the latter, complexes of the type $[Cu(N^N)(POP)]^+$ and $[Cu(N^N)(xantphos)]^+$ are particularly under investigation with N^N usually being a derivative of 2,2'-bipyridine (bpy) or 1,10-phenanthroline (phen), POP = bis(2-(diphenylphosphino)phenyl)ether, xantphos = 4,5-bis(diphenylphosphino)-9,9-dimethylxanthene.[3,4,5,6,7,8,9,10,11,]

Despite the lower abundance and higher price of silver compared to copper, silver(I) complexes are also gaining attention. Heteroleptic silver(I) complexes with N^N and P^P-chelating ligands exhibit promising emissive properties[12] including thermally activated delayed fluorescence (TADF)[13] and have recently been applied as luminophores in light-emitting electrochemical cells[14] and also as UV-absorbing luminescent down-shifters for organic solar cells[15]. With its rigid alkyne backbone, bis(diphenylphosphino)ethyne (dppa, Scheme 1) is a typical bridging ligand. Complexes with a range of metals have been reported, for example with Pt, Pd, Ni, Mo Ru, Cu or Re.[16] While the phosphane ligand typically acts as σ-donor through phosphorus, there are few examples where dppa exhibits side-on coordination via the alkyne bridge.[17,18] For copper, a few dinuclear complexes with a combination of bridging dppa and N^N chelating ligands are already known, for example $[Cu_2(dppa)_2(N^N)_2]^{2+}$ cations where N^N is a substituted bpy,[19] a substituted phen,[20] di-2-pyridyl ketone[21] or 2,4,6-tris(2-pyridyl)-1,3,5-triazine.[22] For silver(I), complex cations with N^N chelating ligands and bridging phosphanes other than dppa are known, some of them exhibiting luminescent properties[23] or being subject to self-assembly into coordination polymers[24] or networks.[25] While analogous $[Ag_2(dppa)_n(N^N)_2]^{2+}$ cations (n = 1–3) are not, to our knowledge, known, dinuclear complexes with one, two or three dppa bridges between the silver(I) cations, but without additional ligands have been investigated by James *et al.*.[26] The characterization of silver(I) phosphane complexes is greatly aided by the use of NMR spectroscopy including heteronuclear low temperature NMR spectroscopy and ^{31}P-^{109}Ag HSQC experiments, which provide invaluable insights when it comes to the characterization of these coordination compounds and their dynamic processes in solution. In order to apply these HSQC NMR techniques, a measurable spin-spin coupling between the abundant nucleus (in this case ^{31}P) and ^{109}Ag is required. A tendency for fast ligand exchange in solution, which results in the removal of the indirect coupling between ^{109}Ag and the other nucleus, can be avoided by using low measurement temperatures[27]. Inspiring examples for ^{109}Ag NMR studies of complexes in solution have been published by Berners-Price *et al.*[28] who studied monomeric, dimeric and

trimeric silver(I) complexes with the 1,2-bis(di-2-pyridylphosphino)ethane ligand and Pregosin *et al.*[29] who investigated the coordination of $Ag(CF_3SO_3)$ by a chiral ferrocenylphosphine ligand.

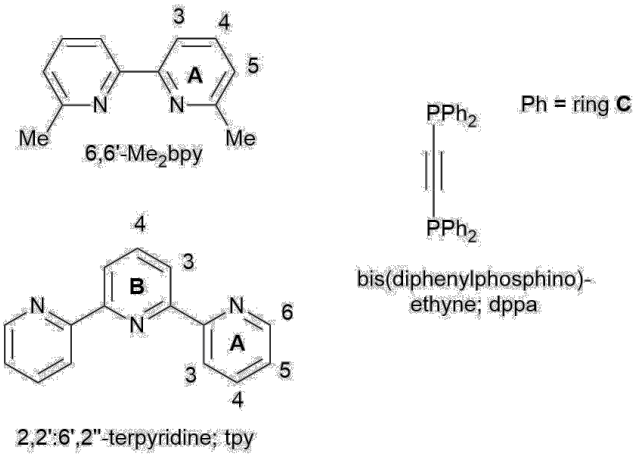

Scheme 1. Structures of applied ligands with ring and atom labels for NMR spectroscopic assignments.

Experimental

General. ^{1}H, ^{13}C and ^{31}P NMR spectra were recorded using a Bruker Avance III-600, III-500 or III-400 NMR spectrometer and direct observe BBFO (600 and 400 MHz) or indirect detection BBI probes (500 MHz). All probes were equipped with self-shielded *z*-gradients. The ^{31}P{^{1}H}-^{109}Ag HSQC spectra were recorded on a triple resonance ^{1}H/^{31}P/low-gamma nucleus indirect TBI probe tuned to 600.132, 242.937 and 27.927 MHz (^{1}H, ^{31}P and ^{109}Ag). The 90° pulse length was 12.5 µs for ^{31}P and 45 µs for ^{109}Ag and the sweep widths 25 and 300 ppm respectively. The experiment was acquired with a modified phase-sensitive HSCQ sequence using 2k (128) data points in the F2 (F1) dimension resulting in an acquisition time of 166 ms (7.6 ms) following a hypercomplex States-TPPI scheme. Suitable ^{1}J coupling constants were converted to 1/4J delays in both INEPT periods. While WALTZ-16 proton decoupling was always applied, the HSQC was recorded with or without GARP ^{109}Ag decoupling during t2 and with or without a 180° ^{31}P refocusing pulse during t1 evolution, thus yielding a set of four HSQC spectra: *J*-coupling in F1 and F2 (four cross peaks), only in F1 (two cross peaks), only in F2 (two cross peaks) and fully decoupled (one cross peak). Typical experiment times were between 15 min and 1h. ^{1}H and ^{13}C NMR chemical shifts were referenced to residual solvent peaks with respect to δ(TMS) = 0 ppm and ^{31}P NMR chemical shifts with respect to δ(85% aqueous H_3PO_4) = 0 ppm. ^{109}Ag chemical shifts were referenced to a solution of $AgNO_3$ (9.1 M) and $Fe(NO_3)_3$ (0.24 M) in D_2O (−47 ppm).[30] The sample temperature in the low temperature NMR experiments was calibrated using a 4% MeOH in CD_3OD sample. The ^{31}P and ^{31}P{^{1}H} NMR spectra were referenced to the signal of $[PF_6]^-$ with δ(septet) = −144.234 ppm where possible. Coalescence temperatures T_c were estimated by interpolation of the line widths of ^{31}P resonances and free activation enthalpies were obtained from T_c using the Eyring equation. Electrospray ionization (ESI) mass spectra were recorded on a Bruker esquire 3000plus. 2,2':6',2"-Terpyridine was either purchased from TCI chemicals or prepared following literature methods with the NMR spectroscopic data matching those reported.[31] $Ag[PF_6]$ and 6,6'-dimethyl-2,2'-bipyridine (6,6'-Me_2bpy) were purchased from Fluorochem and Angene respectively, and dppa from Acros Organics. All commercial chemicals were used as received.

$[Ag_2(dppa)_2(6,6'\text{-}Me_2bpy)_2][PF_6]_2$.

A solution of dppa (49 mg, 0.125 mmol, 2.0 eq) and 6,6'-Me_2bpy (23 mg, 0.125 mmol, 2.0 eq) in CH_2Cl_2 (20 ml) was added to a solution of $Ag[PF_6]$ (32 mg, 0.125 mmol, 2.0 eq) in CH_2Cl_2 (20 mL). The colourless solution was stirred for 2 h, filtered and the filtrate evaporated to dryness. The solid residue was redissolved in CH_2Cl_2 (2 mL) and layered with Et_2O. This yielded colourless crystals which were identified as $[Ag_2(dppa)_2(6,6'\text{-}Me_2bpy)_2][PF_6]_2$ (98 mg, 0.059 mmol, 94%). ^{1}H NMR (500 MHz, $(CD_3)_2CO$, 298 K) δ/ppm 8.38 (d, J = 8.0 Hz, 4H, H^{A3}), 8.11 (t, J = 7.8 Hz, 4H, H^{A4}), 7.62 – 7.52 (m, 24H, H^{C2+C4}), 7.47 (d, J = 7.6 Hz, 4H, H^{A5}), 7.42 – 7.36 (m, 16H, H^{C3}), 2.33 (s, 12H, H^{Me}). ^{13}C NMR (126 MHz, $(CD_3)_2CO$, 298 K) δ/ppm 159.2 (C^{A6}), 153.2 (C^{A2}), 140.9 (C^{A4}), 133.0 (d, J_{PC} = 18 Hz, C^{C2}), 132.5 (C^{C4}), 130.8 (half of d, $J \approx$ 20 Hz, C^{C1}), 130.7 (d, J_{PC} = 10 Hz, C^{C3}), 126.5 (C^{A5}), 121.7 (C^{A3}), 27.5 (C^{Me}). ^{31}P NMR (162 MHz, $(CD_3)_2CO$, 295 K) δ/ppm −22.9 (broad, FWHM = 57 Hz). NMR (208 K): ^{1}H NMR (600 MHz, $(CD_3)_2CO$, 208 K) δ/ppm 8.52 (d, J = 7.8 Hz, 4H, H^{A3}), 8.18 (t, J = 7.7 Hz, 4H, H^{A4}), 7.61 – 7.54 (m, 24H, H^{C2+C4}), 7.49 (d, J = 7.6 Hz, 4H, H^{A5}), 7.37 (t, J = 7.4 Hz, 16H, H^{C3}), 2.16 (s, 12H, H^{Me}). ^{31}P{^{1}H} NMR (243 MHz, $(CD_3)_2CO$, 208 K) δ/ppm −21.5 (d, $^{1}J_{31P\text{-}109Ag}$ = 406.6 Hz, $[Ag_2(dppa)_2(6,6'\text{-}Me_2bpy)_2]^{2+}$), −22.9 (d, $^{1}J_{31P\text{-}107Ag}$ = 352.6 Hz, $[Ag_2(dppa)_2(6,6'\text{-}Me_2bpy)_2]^{2+}$). ESI MS: m/z 685.05 $[Ag(dppa)(6,6'\text{-}Me_2bpy)]^+$ (base peak, calc. 685.11). Found: C, 54.60; H, 4.23; N, 3.75; $C_{76}H_{64}Ag_2F_{12}N_4P_6$ requires C, 54.89; H, 3.88; N, 3.37%.

$[Ag_2(dppa)_2(tpy)_2][PF_6]_2$.

A solution of dppa (39 mg, 0.097 mmol, 2.0 eq) and tpy (23 mg, 0.097 mmol, 2.0 eq) in CH_2Cl_2 (50 ml) was added to a solution of $Ag[PF_6]$ (25 mg, 0.097 mmol, 2.0 eq) in CH_2Cl_2 (30 mL).The pale yellow solution was stirred for 2 h, filtered and the filtrate evaporated to dryness. This yielded pale yellow solid which was identified as $[Ag_2(dppa)_2(tpy)_2][PF_6]_2$ (82 mg, 0.047 mmol, 94 %). ^{1}H NMR (500 MHz, $(CD_3)_2CO$, 298 K) δ/ppm 8.55 (d, J = 7.9 Hz, 4H, H^{B3}), 8.44 (d, J = 8.0 Hz, 4H, H^{A3}), 8.39 (t, J = 7.8 Hz, 2H, H^{B4}), 8.17 (broad signal, 4H, H^{A6}), 7.98 (td, J = 7.8, 1.7 Hz, 4H, H^{A4}), 7.48 (m, 16H, H^{C2}), 7.45 (m, 8H, H^{C4}), 7.26 (t, J = 7.7 Hz, 16H, H^{C3}), 7.01 (broad signal, 4H, H^{A5}). ^{13}C NMR (126 MHz, $(CD_3)_2CO$, 298 K) δ/ppm 154.2 (C^{B2}), 153.5 (C^{A2}), 150.8 (C^{A6}), 141.3 (C^{B4}), 139.6 (C^{A4}), 133.0 (d, J = 18.0 Hz, C^{C2}), 132.0 (C^{C4}), 131.6 (d, J = 26.9 Hz, C^{C1}), 130.4 (d, J = 9.7 Hz, C^{C3}), 126.0 (C^{A5}), 124.2 ($C^{B3/A3}$), 124.1 ($C^{B3/A3}$). ^{31}P{^{1}H} NMR (162 MHz, $(CD_3)_2CO$, 296 K) δ/ppm

−22.9 (broad, FWHM = 110 Hz). NMR (208 K): ^{1}H NMR (600 MHz, $(CD_3)_2CO$, 208 K) δ/ppm 8.65 (d, J = 7.9 Hz, 4H, H^{B3}), 8.51 – 8.47 (m, 6H, H^{A3+B4}), 8.02 – 7.98 (m, 8H, H^{A4+A6}), 7.49 (q, J = 6.6 Hz, 16H, H^{C2}), 7.45 (t, J = 7.4 Hz, 8H, H^{C4}), 7.26 (t, J = 7.5 Hz, 16H, H^{C3}), 6.88 – 6.84 (m, 4H, H^{A5}). $^{31}P\{^{1}H\}$ NMR (243 MHz, $(CD_3)_2CO$, 208 K) δ/ppm −23.0 (d, $^{1}J_{31P\text{-}109Ag}$ = 410.6 Hz, $[Ag_2(dppa)_2(tpy)_2]^{2+}$), −23.0 (d, $^{1}J_{31P\text{-}107Ag}$ = 355.7 Hz, $[Ag_2(dppa)_2(tpy)_2]^{2+}$). ESI MS: *m/z* 734.00 $[Ag(dppa)(tpy)]^{+}$ (base peak, calc. 734.10). Found: C, 55.92; H, 3.87; N, 4.90; $C_{82}H_{62}Ag_2F_{12}N_6P_6$ requires C, 55.93; H, 3.55; N, 4.77%.

$[Ag_2(dppa)(6,6'\text{-}Me_2bpy)_2][PF_6]_2$.

A solution of dppa (19.5 mg, 0.05 mmol, 1.0 eq) and 6,6'-Me_2bpy (18.4 mg, 0.10 mmol, 2.0 eq) in CH_2Cl_2 (15 ml) was added to a solution of $Ag[PF_6]$ (25.3 mg, 0.10 mmol, 2.0 eq) in CH_2Cl_2 (15 mL). The colourless solution was stirred for 2 h and all volatiles were removed in vacuo. This yielded a colourless powder (49 mg, 0.039 mmol, 78 %) which was identified as $[Ag_2(dppa)(6,6'\text{-}Me_2bpy)_2][PF_6]_2$. ^{1}H NMR (500 MHz, $(CD_3)_2CO$, 298 K) δ/ppm 8.40 (d, J = 8.0 Hz, 4H, H^{A3}), 8.13 (t, J = 7.8 Hz, 4H, H^{A4}), 8.01 – 7.95 (m, 8H, H^{C2}), 7.69 – 7.65 (m, 4H, H^{C4}), 7.63 – 7.58 (m, 12H, H^{A5+C3}), 2.66 (s, 12H, CH_3). ^{13}C NMR (126 MHz, $(CD_3)_2CO$, 295 K) δ/ppm 159.3 (C^{A6}), 152.4 (C^{A2}), 141.2 (C^{A4}), 133.8 (d, J = 18.2 Hz, C^{C2}), 133.0 (d, J = 2.1 Hz, C^{C4}), 131.6 (d, J = 11.2 Hz, C^{C1}), 130.8 (d, J = 11.6 Hz, C^{C3}), 126.6 (C^{A5}), 121.1 (C^{A3}), 104.1 (dd, J = 49.3, 4.4 Hz, C^{ethyne}), 27.6 (CH_3). ^{31}P NMR (162 MHz, $(CD_3)_2CO$, 295 K) δ/ppm −16.5 (broad FWHM = 60 Hz). NMR (208 K): $^{31}P\{^{1}H\}$ NMR (243 MHz, $(CD_3)_2CO$, 208 K) δ/ppm −16.1 (d, $^{1}J_{31P\text{-}109Ag}$ = 714.6 Hz, $[Ag_2(dppa)(6,6'\text{-}Me_2bpy)_2]^{2+}$), −16.1 (d, $^{1}J_{31P\text{-}109Ag}$ = 619.1 Hz, $[Ag_2(dppa)(6,6'\text{-}Me_2bpy)_2]^{2+}$),−16.4 (d, $^{1}J_{31P\text{-}107Ag}$ = 711.1 Hz, $[Ag_2(dppa)(6,6'\text{-}Me_2bpy)_2]^{2+}$, second conformer), −16.4 (d, $^{1}J_{31P\text{-}109Ag}$ = 615.5 Hz, $[Ag_2(dppa)(6,6'\text{-}Me_2bpy)_2]^{2+}$, second conformer).

$[Ag_2(dppa)(tpy)_2][PF_6]_2$.

$AgPF_6$ (12.6 mg, 0.05 mmol, 2.0 eq), dppa (9.9 mg, 0.025 mmol, 3.0 eq) and terpy (11.5 mg, 0.05 mmol, 2.0 eq) were weighted into a round bottom flask. Acetone-d^6 (4 ml) was added and the solution was stirred for 2h. NMR spectra were recorded and the signals assigned where possible. Identified species in solution are $[Ag_2(dppa)(tpy)_2][PF_6]_2$ and $[Ag_2(dppa)_2(tpy)_2][PF_6]_2$ plus unidentified side products. Room temperature NMR: ^{1}H NMR (500 MHz, $(CD_3)_2CO$, 298 K) δ/ppm 8.53 (d, J = 7.9 Hz, 4H, H^{B3}), 8.44 (dt, J = 8.1, 0.8 Hz, H^{A3}), 8.38 (t, J = 7.9 Hz, 2H, H^{B4}), 8.38 – 8.34 (broad signal, FWHM = 13 Hz, 4H, H^{A6}), 8.00 (td, J = 7.8 Hz, 4H, H^{A4}), 7.70 – 7.59 (broad signal, FWHM = 25 Hz, 8H, H^{C2}), 7.53 (t, J = 7.3 Hz, 4H, H^{C4}), 7.39 (t, J = 6.8 Hz, 8H, H^{C3}), 7.26 (broad signal, FWHM = 18 Hz, 4H, H^{A5}). ^{13}C NMR (126 MHz, $(CD_3)_2CO$, 298 K) δ/ppm 153.7, 153.1, 151.3 (C^{A6}), 141.5 (C^{B4}), 139.8 (C^{A4}), 133.3 (d, J = 20.6 Hz, C^{C2}), 132.4 (C^{C4}), 130.5 (d, J = 10.9 Hz, C^{C3}), 126.3 (C^{A5}), 124.2 (C^{B3}), 124.0 (C^{A3}). $^{31}P\{^{1}H\}$ NMR (162 MHz, $(CD_3)_2CO$, 296 K) δ/ppm −21.4 (broad, FWHM = 140 Hz). Low temperature NMR (208 K): $^{31}P\{^{1}H\}$ NMR (243 MHz, $(CD_3)_2CO$, 208 K) δ/ppm −20.6 (d, $^{1}J_{31P\text{-}109Ag}$ = 657.8 Hz, $[Ag_2(dppa)(tpy)_2]^{2+}$), −20.6 (d, $^{1}J_{31P\text{-}107Ag}$ = 572.8 Hz, $[Ag_2(dppa)(tpy)_2]^{2+}$), −23.0 (d, $^{1}J_{31P\text{-}109Ag}$ = 410.4 Hz, $[Ag_2(dppa)_2(tpy)_2]^{2+}$), −23.0 (d, $^{1}J_{31P\text{-}107Ag}$ = 355.8 Hz, $[Ag_2(dppa)_2(tpy)_2]^{2+}$).

Crystallography. Data were collected on a Bruker Kappa Apex2 diffractometer with data reduction, solution and refinement using the programs APEX[32] and CRYSTALS.[33] Structural analysis was carried out using Mercury v. 3.7.[34,35]

$[Ag_2(dppa)(6,6'\text{-}Me_2bpy)_2][PF_6]_2\cdot Et_2O$.

$C_{53}H_{50}Ag_2F_{12}N_4O_1P_4$, M = 1326.61, colourless block, triclinic, space group $P\bar{1}$, a = 11.4217(7), b = 15.4399(10), c = 16.5048(10) Å, α = 90.991(2), β = 107.581(2), γ = 101.888(2)°, U = 2705.3(3) Å^3, Z = 2, D_c = 1.628Mg m^{-3}, μ(Cu-Kα) = 7.666 mm^{-1}, T = 123 K. Total 20062 reflections, 9500 unique, R_{int} = 0.021. Refinement of 9089 reflections (685 parameters) with I >2σ(I) converged at final R_1 = 0.0350 (R_1 all data = 0.0366), wR_2 = 0.0806 (wR_2 all data = 0.0810), gof = 0.9224. CCDC 1580157.

$[Ag_2(dppa)_2(tpy)_2][PF_6]_2\cdot 2(CD_3)_2CO$ (pseudo-polymorph 1).

$C_{88}H_{74}Ag_2F_{12}N_6O_2P_6$, M = 1877.15, colourless block, triclinic, space group $P\bar{1}$, a = 12.1355(10), b = 12.5994(10), c = 14.8038(12) Å, α = 95.415(3), β = 112.162(3), γ = 93.696(3)°, U = 2074.6(3) Å^3, Z = 1, D_c = 1.502Mg m^{-3}, μ(Cu-Kα) = 5.556 mm^{-1}, T = 123 K. Total 20395 reflections, 7245 unique, R_{int} = 0.033. Refinement of 6529 reflections (523 parameters) with I >2σ(I) converged at final R_1 = 0.0258 (R_1 all data = 0.0291), wR_2 = 0.0283 (wR_2 all data = 0.0316), gof = 1.0823. CCDC 1580158.

$[Ag_2(dppa)_2(tpy)_2][PF_6]_2\cdot CH_2Cl_2$ (pseudo-polymorph 2).

$C_{83}H_{64}Ag_2Cl_2F_{12}N_6P_6$, M = 1845.93, yellow block, monoclinic, space group $P2_1/c$, a = 23.7942(10), b = 30.1578(13), c = 44.766(2) Å, α = 90, β = 95.386(2), γ = 90°, U = 31981(2) Å^3, Z = 16, D_c = 1.533 Mg m^{-3}, μ(Cu-Kα) = 6.338 mm^{-1}, T = 123 K. Total 226517 reflections, 59009 unique, R_{int} = 0.045. Refinement of 52995 reflections (4015 parameters) with I >2σ(I) converged at final R_1 = 0.0614 (R_1 all data = 0.0699), wR_2 = 0.1030 (wR_2 all data = 0.1046), gof = 0.8961. CCDC 1580159.

Results and discussion

Synthesis and NMR spectroscopic characterization

The Ag^+ cation is known to accommodate a wider range of coordination numbers (two to six) than Cu^+, which prefers to adopt a tetrahedral coordination geometry. Previously reported dinuclear species containing copper(I) and bridging dppa combined with an N^N chelating ligand feature a doubly-bridged $\{Cu_2(dppa)_2\}$ motif.[19,20,21,22] For an initial investigation of the reaction of Ag^+ with dppa and N^N ligands, we chose a combination of one chelating and one bridging ligand per Ag^+.

Reaction of $Ag[PF_6]$, 6,6'-Me_2bpy and dppa in a 1 : 1 : 1 ratio resulted in the isolation of a colourless crystalline solid. Preliminary structural data from single-crystal X-ray diffraction (see later) confirmed the doubly-bridged dimeric structure of $[Ag_2(dppa)_2(6,6'\text{-}Me_2bpy)_2][PF_6]_2$ (Scheme 2). Elemental analysis was consistent with $\{[Ag(dppa)(6,6'\text{-}Me_2bpy)][PF_6]\}_n$

and in the positive mode electrospray (ESI) mass spectrum, the base peak at *m/z* 685.05 arose from $[Ag(dppa)(6,6'\text{-}Me_2bpy)]^+$. No higher mass peaks were observed.

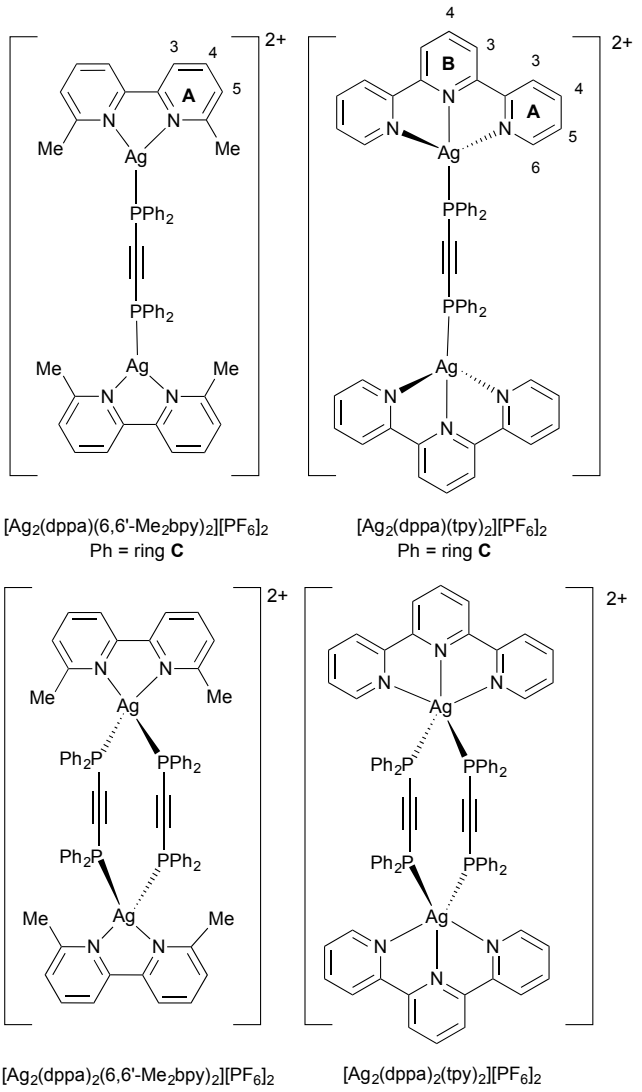

Scheme 2. Structures of dinuclear complexes with one and two dppa bridges; ring and atom labels for NMR spectroscopic assignments.

Solid $[Ag_2(dppa)_2(6,6'\text{-}Me_2bpy)_2][PF_6]_2$ was dissolved in acetone-d_6 and the room temperature ^{1}H NMR solution spectrum showed one set of signals, with the integrals consistent with a 1 : 1 ratio of 6,6'-Me_2bpy : dppa. An indicator for the formation of the $[Ag_2(dppa)_2(6,6'\text{-}Me_2bpy)_2]^{2+}$ cation was a cross peak in the NOESY spectrum between the methyl groups of 6,6'-Me_2bpy and the H^{C2} protons of the phenyl rings of dppa (Fig. S1† and S2†, see Scheme 2 for atom labelling). On lowering the temperature from 298 to 208 K, no additional signals appeared in the ^{1}H NMR spectrum although some shifting of resonances including that of the H^{Me} protons in 6,6'-Me_2bpy were observed (Fig. S3†). The solution $^{31}P\{^1H\}$ NMR spectrum at 298 K showed a septet for $[PF_6]^-$ and a signal at δ −21.1 ppm (FWHM = 38 Hz) arising from dppa. Upon cooling the sample from 298 to 208 K, the ^{31}P NMR resonance split into two doublets centred at δ −21.5 ppm (Fig. 1). The latter result from coupling to ^{109}Ag and ^{107}Ag, with coupling constants of 407 Hz ($^1J_{31P\text{-}109Ag}$) and 353 Hz ($^1J_{31P\text{-}107Ag}$), respectively (Fig. 2).

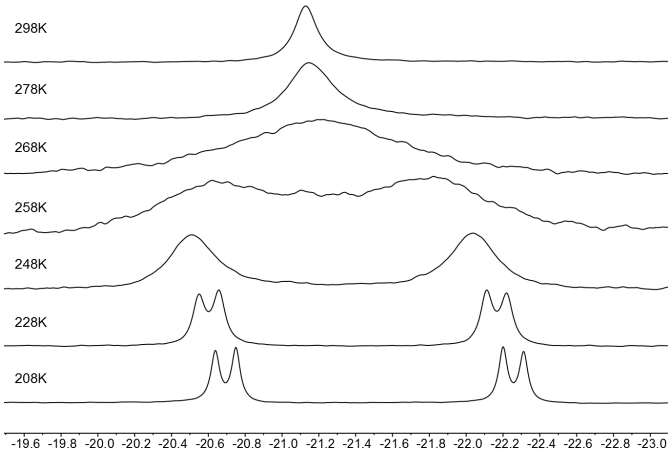

Fig. 1. Variable temperature (243 MHz) $^{31}P\{^1H\}$ NMR spectra of $[Ag_2(dppa)_2(6,6'\text{-}Me_2bpy)_2][PF_6]_2$ in $(CD_3)_2CO$.

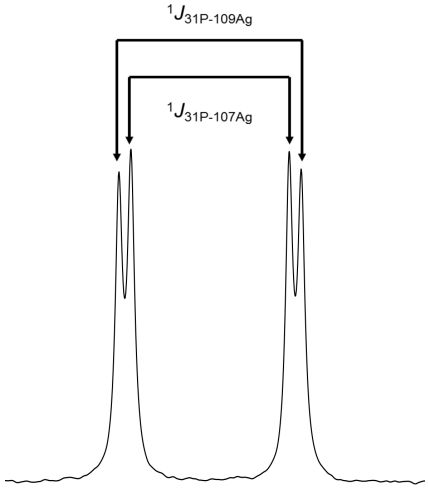

Fig. 2. Illustration of the two doublets and the two coupling constants $^1J_{31P\text{-}109Ag}$ and $^1J_{31P\text{-}107Ag}$ in the 243 MHz $^{31}P\{^1H\}$ NMR spectrum of $[Ag_2(dppa)_2(6,6'\text{-}Me_2bpy)_2][PF_6]_2$ in $(CD_3)_2CO$ at 208 K.

The $^{31}P\{^1H\}$-^{109}Ag HSQC spectrum was recorded at 228 K and is shown in Fig. 3. The $^{109}Ag\{^{31}P\}$ NMR projection is plotted in the vertical dimension (F1) and the $^{31}P\{^1H\}$ NMR spectrum in the horizontal dimension (F2). Depending on the additional decoupling (none, $\{^{31}P\}$, $\{^{109}Ag\}$, or both $\{^{31}P\}$ and $\{^{109}Ag\}$), a different number of cross peaks results. The chemical shift of the ^{109}Ag NMR signal is at δ 1161 ppm with a splitting of 816 Hz in the F1 dimension (^{109}Ag) and a coupling constant of 407 Hz in the F2 (^{31}P) dimension. While for a heteronuclear two-spin AX spin system, the distances between the cross peaks in the fully or partially coupled spectra are always equal to the ^1J(AX) coupling constant in F1 and F2, it can be shown elegantly by the product operator formalism, that

for a heteronuclear three-spin AX_2 spin system (I_{1z}, I_{2z}, $S_{3z;}$ $^1J_{13}$ = $^1J_{23}$) the modulation of the pure in-phase terms at the end of the HSQC sequence before the final t_2 evolution can be written as:[36]

$$\cos(2 J_{13} \pi t_1)\cos(\Omega_3 t_1)(I_{1x} + I_{2x})$$

which is equivalent to:

$$\tfrac{1}{2} (\cos((\Omega_3 \pm 2 J_{13} \pi) t_1)(I_{1x} + I_{2x})$$

This explains the spacing of the two resonances in F1 by two times the coupling constant $^1J_{31P\text{-}109Ag}$. It is, therefore, of additional analytical value to record the $^{31}P\{^1H\}$-^{109}Ag HSQC spectrum without decoupling in F2 and F1, as the doubling of the splitting constant in F1 unambiguously discriminates between an AX and an AX_2 spin system and allows, in combination with the ^{109}Ag chemical shift and the range of the $^1J_{31P\text{-}109Ag}$ coupling constant, a detailed description of the number of bridging ligands in solution. The doubling of the splitting constants as a result of two attached phosphorus atoms at one silver centre has also been reported by Pregosin *et al.*.[29] From this part of the investigation, we were able to conclude that the $[Ag_2(dppa)_2(6,6'\text{-}Me_2bpy)_2]^{2+}$ complex remains intact in solution and does not undergo any ligand redistributions.

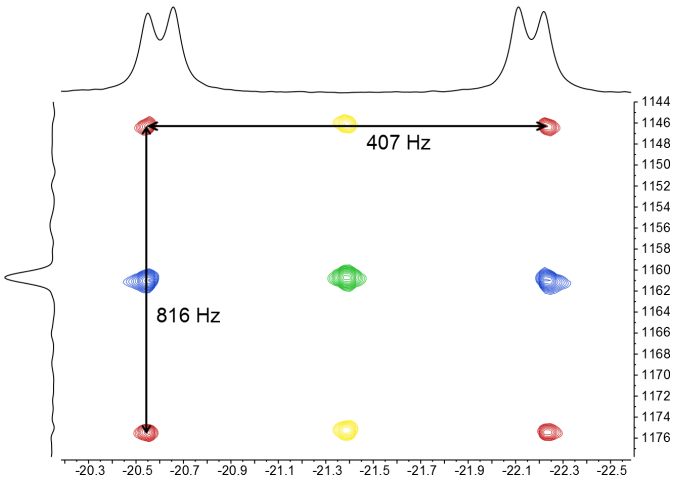

Fig. 3. $^{31}P\{^1H\}$-^{109}Ag HSQC spectrum of $[Ag_2(dppa)_2(6,6'\text{-}Me_2bpy)_2][PF_6]_2$ in $(CD_3)_2CO$ at 228 K. Cross peaks without decoupling are coloured in red, with $\{^{31}P\}$ decoupling in blue, with $\{^{109}Ag\}$ decoupling in yellow, and with both $\{^{31}P\}$ and $\{^{109}Ag\}$ decoupling green.

Following from the investigation of the assembly process involving a 1 : 1 : 1 mixture of $Ag[PF_6]$, 6,6'-Me_2bpy and dppa, we turned our attention to a 1 : 1 : 1 combination of $Ag[PF_6]$, tpy and dppa. X-ray quality crystals were grown by layering Et_2O over a concentrated solution of the compound in CH_2Cl_2 and a second set of crystals grew in an NMR sample of the compound in acetone-d_6 after few days. The structures of two pseudo-polymorphs of $[Ag_2(dppa)_2(tpy)_2][PF_6]_2$ (differing in solvate) are described later. Elemental analysis for thebulk material was in agreement with $\{[Ag(dppa)(tpy)][PF_6]\}_n$ and the dominant peak envelope in the electrospray mass spectrum (positive mode) at *m/z* 734.0 corresponded to $[Ag(dppa)(tpy)]^+$.

Solid $[Ag_2(dppa)_2(tpy)_2][PF_6]_2$ was dissolved in acetone-d_6 and the solution room temperature ^1H NMR spectrum was recorded. The relative integrals of the signals were in accord with a 1 : 1 ratio of tpy : dppa, and with one environment for each ligand. As in the reaction with 6,6'-Me_2bpy, the NOESY spectrum provided valuable information (Fig. S4† and S5†). At 208 K, a NOESY cross peak between the H^{A6} proton at tpy and the phenyl H^{C2} protons of dppa was consistent with the Ag^+ ion being bound to both ligands. This, along with confirmation of the 1 : 1 : 1 ratio of $Ag[PF_6]$, tpy and dppa was consistent with the presence of a dimer in solution. No additional signals appeared in the ^1H NMR spectrum on cooling from 298 to 208 K. The shifts of the signals for the dppa protons were little affected on cooling and the signals of the tpy protons H^{A3}, H^{A4}, H^{B3} and H^{B4} were shifted to higher frequency. In contrast, the signals for H^{A5} and H^{A6} shifted towards lower frequency (Fig. S6†). The spectroscopic signature for the tpy was consistent with either a tridentate bonding mode, or a bidentate mode undergoing fast exchange between two equivalent sites.[37] The symmetry of the tpy unit is maintained on the NMR timescale on going from 298 to 208 K, but the coordination mode of the tpy ligand in solution remains ambiguous. The chelating nature of tpy in the solid-state structure of $[Ag_2(dppa)_2(tpy)_2]^{2+}$ is discussed later.

In addition to the septet for $[PF_6]^-$, a signal at δ −22.9 ppm (FWHM = 110 Hz) was observed in the room temperature ^{31}P NMR spectrum. Cooling from 298 to 208 K leads to a splitting of this signal into two doublets centred at δ −23.0 ppm with coupling constants of 411 Hz ($^1J_{31P\text{-}109Ag}$) and 356 Hz ($^1J_{31P\text{-}107Ag}$), respectively (Fig. 4). The $^{31}P\{^1H\}$-^{109}Ag spectrum was recorded at 208 K and is illustrated in Fig. S7†. Both the shift of the ^{109}Ag signal (δ 1154 ppm) and the coupling constants in the F2 and F1 dimensions ($^1J_{31P\text{-}109Ag}$ and $^1J_{109Ag\text{-}31P}$, with $^1J_{109Ag\text{-}31P}$ being doubled again), are very similar: 411 and 840 Hz respectively for $[Ag_2(dppa)_2(tpy)_2]^{2+}$ and 407 and 816 Hz respectively for $[Ag_2(dppa)_2(6,6'\text{-}Me_2bpy)_2]^{2+}$ (Table 1). This is consisent with similar structures. The data are consistent with the retention of $[Ag_2(dppa)_2(tpy)_2]^{2+}$ in solution.

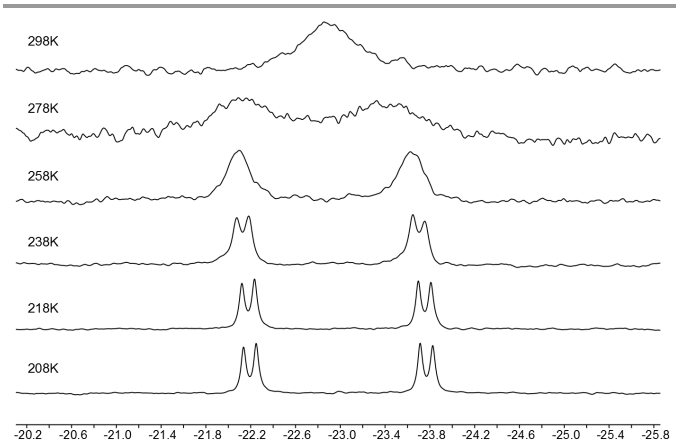

Fig. 4. Variable temperature 243 MHz $^{31}P\{^1H\}$ NMR spectra of $[Ag_2(dppa)_2(tpy)_2][PF_6]_2$ in $(CD_3)_2CO$.

Table 1. Overview of NMR chemical shifts and coupling constants (208 K).

Cation	$[Ag_2(dppa)(6,6'\text{-}Me_2bpy)_2]^{2+}$	$[Ag_2(dppa)(tpy)_2]^{2+}$	$[Ag_2(dppa)_2(6,6'\text{-}Me_2bpy)_2]^{2+}$	$[Ag_2(dppa)_2(tpy)_2]^{2+}$
N^N	bpy	tpy	bpy	tpy
Number of dppa bridges	1	1	2	2
δ (^{109}Ag) /ppm	735	765	1161	1154
δ (^{31}P) /ppm	−16.1	−20.6	−21.5	−23.0
$^1J_{31P\text{-}109Ag}$ /Hz	715	658	407	411
splitting F1 /Hz	716	666	816	840
$T_{coalesc}$ / K	286 (3)	278 (2)	262 (2)	287 (3)
$\Delta G^{\ddagger}$ / kJ/mol	52.3 (5)	51.7 (4)	51.0 (4)	48.9 (5)

Previous reports[21,26] confirm that $[Ag_2(dppa)(dppf)_2]^{2+}$ (dppf = 1,1'-bis(diphenylphosphino)ferrocene) and $[Ag_2(dppa)]^{2+}$ both contain single dppa bridges between two Ag(I) centres. We therefore decided to try to force a singly bridged mode by reducing the amount of dppa in the self-assembly process from 1.0 to 0.5 eq with respect to $Ag[PF_6]$. We were curious to see whether the silver cation would be satisfied with threefold coordination or whether it would prefer additional donors, for example by making use of all three *N*-donors of the tpy ligand.

Reaction of $Ag[PF_6]$, 6,6'-Me_2bpy and dppa in a 2 : 2 : 1 ratio yielded a colourless solid. Single crystals were grown from a CH_2Cl_2 solution of the product layered with Et_2O, and X-ray diffraction confirmed the formation of $[Ag_2(dppa)(6,6'\text{-}Me_2bpy)_2][PF_6]_2$ (see later). The ^{1}H NMR spectrum of a solution of the isolated product in acetone-d_6 (298 K) was consistent with coordinated 6,6'-Me_2bpy and dppa ligands in a 2 : 1 ratio. A cross-peak in the NOESY spectrum between the methyl groups of 6,6'-Me_2bpy and the H^{C2} protons of the phenyl rings of dppa (Fig. S8† and S9†) confirmed the presence of an $\{AgN_2P\}$ coordination sphere, indicating the formation of $[Ag_2(dppa)(6,6'\text{-}Me_2bpy)_2]^{2+}$. On decreasing the temperature from 298 to 208 K, a subspectrum appeared in the ^{1}H NMR spectrum (Fig. 5, bottom and S10†) including an additional methyl signal at δ 2.55 ppm. The relative integrals of signals for the major and minor species showed the latter to comprise approximately 20% of the sample. In the ^{31}P NMR spectrum at 298 K, a septet from $[PF_6]^-$ was observed along with a broadened signal (FWHM = 60 Hz) at δ −16.5 ppm from dppa. Upon cooling (Fig. 6), the typical set of two doublets was resolved, centred at δ −16.1 ppm (Table 1), and at 208 K, a second set of doublets centred at δ −16.4 ppm ($^1J_{31P\text{-}109Ag}$ = 711 Hz) was observed. The data suggested that the minor species possessed similar structural properties to the dominant compound. An EXSY cross peak between the two methyl signals (major and minor) in the 208 K NOESY spectrum (Fig. S9†, δ 2.66 and 2.20 ppm), gave strong evidence that the subspectrum belonged not to a compositionally different species, but rather to a second conformer. A possible explanation is that at 208 K, the rotation of the alkyne bridge is slow with respect to the NMR spectroscopic time scale and that different conformers are resolved in the spectrum. The possible conformers are further discussed later.

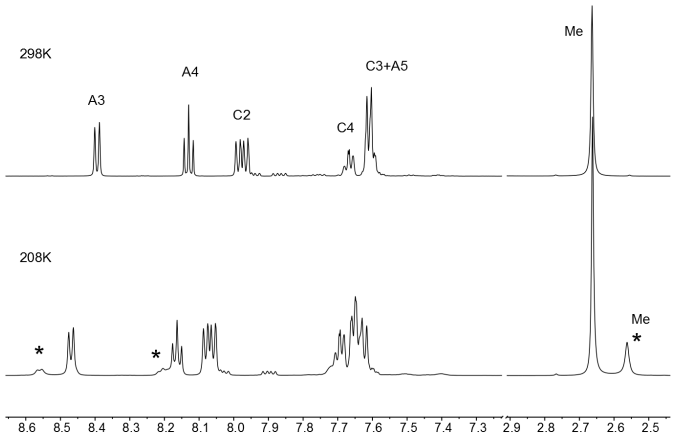

Fig. 5. Part of the ^{1}H NMR spectra of $[Ag_2(dppa)(6,6'\text{-}Me_2bpy)_2][PF_6]_2$ in $(CD_3)_2CO$ at 298 K, 500 MHz (top) and 208 K, 600 MHz (bottom), where a subspectrum is visible. Signals marked with an asterisk indicate the second conformer resolved at low temperature. For the full spectrum see Fig. S10†.

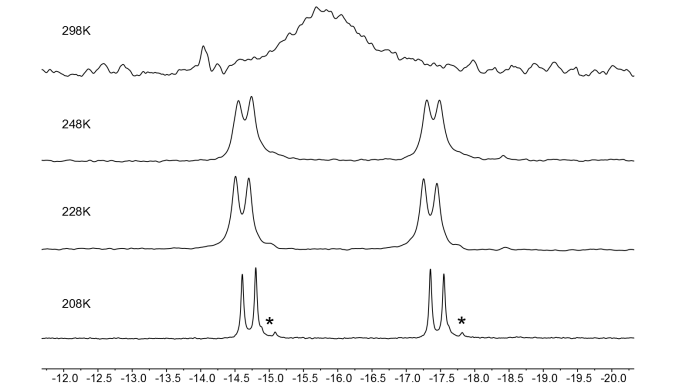

Fig. 6. Variable temperature 243 MHz $^{31}P\{^1H\}$ NMR spectra of $[Ag_2(dppa)(6,6'\text{-}Me_2bpy)_2][PF_6]_2$ in acetone-d_6. Signals marked with an asterisk indicate the smaller doublet assigned to the second conformer resolved at lower temperature.

In the $^{31}P\{^1H\}$-^{109}Ag HSQC spectrum (Fig. 7), the ^{109}Ag signal is centred at δ 735 ppm, resulting in a considerable shift of 426 ppm in comparison to the signal of $[Ag_2(dppa)_2(6,6'\text{-}Me_2bpy)_2][PF_6]_2$ (δ 1161 ppm). Two other significant differences are observed regarding the splitting patterns. The value of $^1J_{31P\text{-}109Ag}$ = 715 Hz for singly-bridged $[Ag_2(dppa)(6,6'\text{-}Me_2bpy)_2]^{2+}$ is significantly larger than $^1J_{31P\text{-}109Ag}$ = 407 Hz for doubly-bridged $[Ag_2(dppa)_2(6,6'\text{-}Me_2bpy)_2]^{2+}$. This is in accordance with James *et al.* who have reported that coupling constants decreased from 767 Hz for singly-bridged

$[Ag_2(dppa)]^{2+}$ to 505 Hz in the doubly-bridged $[Ag_2(dppa)_2]^{2+}$ and to 377 Hz for the triply-bridged $[Ag_2(dppa)_3]^{2+}$.[26,38]

The second difference concerns the coupling of the silver nucleus to ^{31}P. In contrast to the doubly-bridged $[Ag_2(dppa)_2(6,6'\text{-}Me_2bpy)_2]^{2+}$ and $[Ag_2(dppa)_2(tpy)_2]^{2+}$, where the F1 splitting roughly doubles $^1J_{31P\text{-}109Ag}$, the two coupling constants are almost identical for the singly-bridged $[Ag_2(dppa)(6,6'\text{-}Me_2bpy)_2]^{2+}$ (715 Hz for $^1J_{31P\text{-}109Ag}$ and 716 Hz for the splitting in F1).

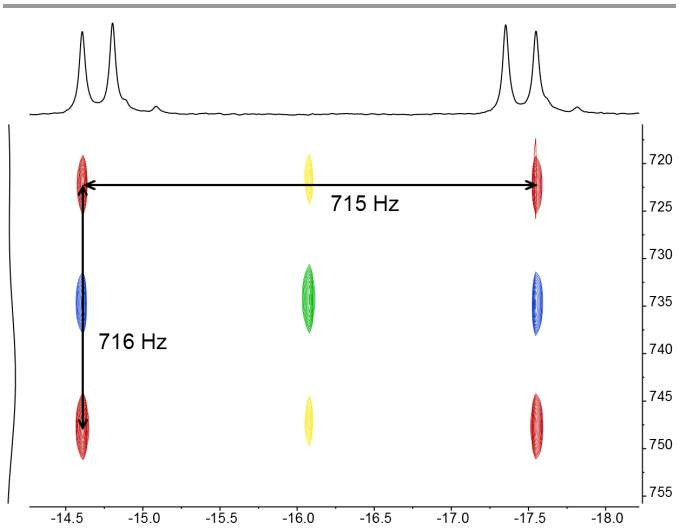

Fig. 7. $^{31}P\{^1H\}$-^{109}Ag HSQC spectrum of $[Ag_2(dppa)(6,6'\text{-}Me_2bpy)_2][PF_6]_2$ in $(CD_3)_2CO$ at 208 K. Cross peaks without decoupling are coloured in red, with $\{^{31}P\}$ decoupling in blue, with $\{^{109}Ag\}$ decoupling in yellow and with both $\{^{31}P\}$ and $\{^{109}Ag\}$ decoupling green.

We next investigated the effects of changing the 6,6'-Me_2bpy ligand for tpy. An acetone-d_6 solution of $Ag[PF_6]$, tpy and dppa in a 2 : 2 : 1 ratio was stirred for 2 hours, concentrated and analysed by NMR spectroscopy. For this reaction, no crystalline product was isolated, and the investigation focused on speciation in the reaction mixture. While the signals for H^{B3}, H^{B4}, H^{A3} and H^{A4} were well resolved at 298 K, those for H^{A5} and H^{A6} as well as the signals of the C-ring protons were broadened (Fig. S13†). A cross peak in the NOESY spectrum (298 K, (Fig. S11†) showed the proximity of the H^{A6} and H^{C2} protons and indicated that Ag^+ was coordinated by both tpy and dppa (Fig. S13†). The dppa ligand gave rise to a broad signal (δ −21.4 ppm, FWHM = 140 Hz) in ^{31}P NMR spectrum at 298 K. Upon cooling, this signal split into two sets of doublets with an integral ratio of 2 : 1 (Fig. 8). The smaller set of doublets centred at δ −20.6 ppm had a value of $^1J_{31P\text{-}109Ag}$ = 658 Hz. This is smaller than, but in the same range as, the coupling constant in $[Ag_2(dppa)(6,6'\text{-}Me_2bpy)_2]^{2+}$ (Table 1). The larger set of doublets was centred at δ −23.0 ppm with $^1J_{31P\text{-}109Ag}$ = 410 Hz. These values indicated the formation of the doubly-bridged $[Ag_2(dppa)_2(tpy)_2]^{2+}$, which was further confirmed by looking at the ^1H NMR and $^{31}P\{^1H\}$-^{109}Ag HSQC spectra at 208 K. The low temperature ^1H NMR spectrum showed nine relatively sharp signals (Fig. 9, top, Fig. S12† and Fig. S13†, bottom). However, the signals were located at different shifts than at room temperature, and in addition eight broad signals were visible. Compared with the low temperature ^1H NMR spectrum of the doubly-bridged $[Ag_2(dppa)_2(tpy)_2]^{2+}$ cation (Fig. 9), the sharp signals are consistent with the signals for $[Ag_2(dppa)_2(tpy)_2]^{2+}$, both in shift and multiplicity, thus confirming the proposal that the dominant species in solution is the doubly-bridged cation.

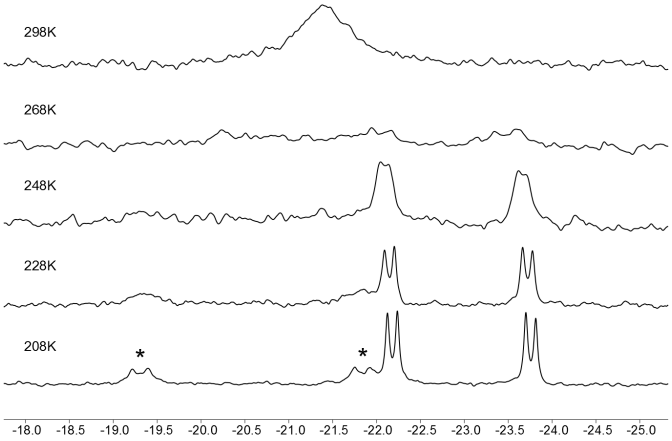

Fig. 8. Variable temperature 243 MHz $^{31}P\{^1H\}$ NMR spectra of a 2:2:1 mixture of $Ag[PF_6]$, tpy and dppa in acetone-d_6. Signals marked with an asterisk indicate the lower intensity resonance assigned to the mono-bridged $[Ag_2(dppa)(tpy)_2]^{2+}$ species resolved at lower temperature.

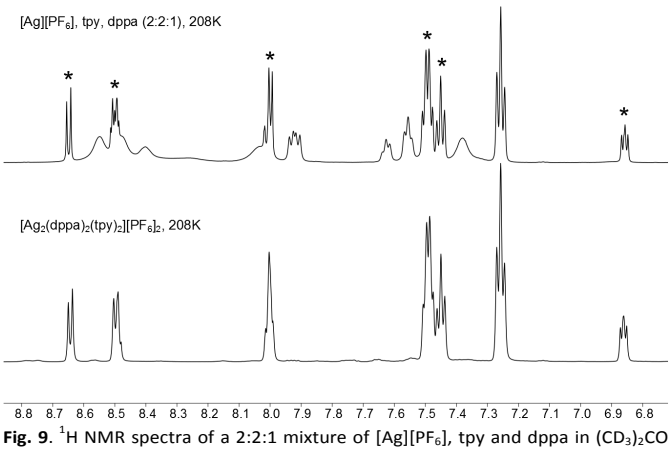

Fig. 9. ^1H NMR spectra of a 2:2:1 mixture of [Ag][PF_6], tpy and dppa in $(CD_3)_2CO$ at 208 K, 600 MHz (top) and of $[Ag_2(dppa)_2(tpy)_2][PF_6]_2$ in $(CD_3)_2CO$ at 298 K, 500 MHz (bottom). Signals in the top spectrum that are in agreement with $[Ag_2(dppa)_2(tpy)_2][PF_6]_2$ are marked with an asterisk.

Some of the remaining signals should then belong to a singly-bridged species. While the set of doublets is shifted to lower frequency with respect to $[Ag_2(dppa)(6,6'\text{-}Me_2bpy)_2][PF_6]_2$ (δ −20.6 ppm versus δ −16.1 ppm), the coupling constants are sufficiently similar to indicate a singly-bridged $[Ag_2(dppa)(tpy)_2]^{2+}$ cation. This is further supported by the $^{31}P\{^1H\}$-^{109}Ag HSQC spectrum (Fig. S14†). With a chemical shift of δ 765 ppm, the ^{109}Ag NMR signal is close to that of the singly-bridged $[Ag_2(dppa)(6,6'\text{-}Me_2bpy)_2]^{2+}$ cation. Furthermore, the coupling constant in the F1 dimension, $^1J_{109Ag\text{-}31P}$, = 666 Hz deviates only slightly from the one observed in

Table 2. Comparison of structural parameters for the silver(I) coordination compounds.

Compound	$[Ag_2(dppa)(6,6'\text{-}Me_2bpy)_2]$	$[Ag_2(dppa)_2(tpy)_2]\cdot 2(CH_3)_2CO$ pseudo-polymorph 1	$[Ag_2(dppa)_2(tpy)_2]\cdot 2CH_2Cl_2$ pseudo-polymorph 2			
			a Ag1Ag2	b Ag3Ag4	c Ag5Ag6	d Ag7Ag8
Number of Ag/unit cell	2	1	8	8	8	8
N^N chelating ligand	6,6'-Me_2bpy	tpy	tpy	tpy	tpy	tpy
Number of dppa bridges	1	2	2	2	2	2
Number of attached N / Number of available N	4 / 4	6 / 6	5 / 6	4 / 6	6 / 6	6 / 6
Denticity	both bidentate	both tridentate	one bidentate (Ag2), one tridentate (Ag1)	both bidentate	both tridentate	both tridentate
Ag–P distances	Ag1–P2 = 2.3475(6); Ag2–P1 = 2.3390(7)	Ag1–P1(2_766) = 2.4608(5); Ag1–P2 = 2.4228(5)	Ag1–P2 = 2.4120(9); Ag1–P4 = 2.4892(9); Ag2–P1 = 2.4341(9); Ag2–P3 = 2.4620(9)	Ag3–P5 = 2.3984(9); Ag3–P8 = 2.4997(9); Ag4–P6 = 2.4086(9); Ag4–P7 = 2.4545(9)	Ag5–P9 = 2.4792(9); Ag5–P12 = 2.4166(9); Ag6–P10 = 2.4760(9); Ag6–P11 = 2.4279(10)	Ag7–P13 = 2.4600(9); Ag7–P16 = 2.4127(9); Ag8–P14 = 2.4830(10); Ag8–P15 = 2.4257(10)
Ag–N distances	Ag1–N1 = 2.278(2); Ag1–N2 = 2.302(2); Ag2–N3 = 2.285(2); Ag2–N4 = 2.249(2)	Ag1–N1 = 2.5179(18); Ag1–N2 = 2.3934(17); Ag1–N3 = 2.5100(18)	Ag1–N1 = 2.481(3); Ag1–N2 = 2.410(3); Ag1–N3 = 2.503(3); Ag2–N4 = 2.389(3); Ag2–N5 = 2.432(3); Ag2–N6 = 2.726(3)[a]	Ag3–N7 = 2.430(3); Ag3–N8 = 2.355(3); Ag3–N9 = 2.762(3)[a]; Ag4–N10 = 2.423(3); Ag4–N11 = 2.377(3); Ag4–N12 = 2.727(3)[a]	Ag5–N13 = 2.580(3); Ag5–N14 = 2.401(3); Ag5–N15 = 2.475(3); Ag6–N16 = 2.542(3); Ag6–N17 = 2.430(3); Ag6–N18 = 2.478(4)	Ag7–N19 = 2.462(3); Ag7–N20 = 2.394(3); Ag7–N21 = 2.533(3); Ag8–N22 = 2.553(4); Ag8–N23 = 2.431(3); Ag8–N24 = 2.454(4)
Dihedral angle Ag–P–P–Ag	108.14(3)	44.24(3)	28.94(4); −36.47(4)	24.91(5); −44.43(4)	40.80(4); −40.86(4)	29.79(5); −45.26(4)
Torsion angle P–C–C–P	21(4)	22(3)	−176(2); −31(7)	105(5); or 18(7)	27(5); 63(6)	−102(5); −39(8)
Tilting angle Ag–P–C	Ag1–P2–C9 = 105.74(9); Ag2–P1–C10 = 116.15(9)	Ag1–P2–C9 = 114.29(7); C10–P1–Ag1(2_766) = 110.65(7)	Ag1–P4–C15 = 112.9(1); Ag1–P2–C3 = 111.0(1); Ag2–P3–C14 = 113.3(1); Ag2–P1–C4 = 109.7(1)	Ag3–P8–C103 = 110.3(1); Ag3–P5–C97 = 109.4(1); Ag4–P7–C102 = 117.4(1); Ag4–P6–C98 = 111.0(1)	Ag5–P12–C197 = 109.5(1); Ag5–P9–C191 = 113.7(1); Ag6–P11–C196 = 114.1(1); Ag6–P10–C192 = 111.6(1)	Ag8–P14–C286 = 112.4(1); Ag8–P15–C290 = 114.3(1); Ag7–P16–C291 = 108.0(1); Ag7–P13–C285 = 113.9(1)
Torsion angles N–C–C–N	−5.2(4); −1.7(4)	−12.1(3); 24.5(3)	19.8(5); −12.4(5); 23.1(5); 7.9(5) (to nonbonding N)	18.7(5); 20.0(5) (to nonbonding N); −6.4(5); −30.9(5) (to nonbonding N)	−16.7(6); 5.9(5); −9.4(5); −17.8(5)	10.3(6); 3.5(6); 22.2(5); −0.4(5)
Biting angles N–Ag–N	73.26(8); 73.64(9)	67.37(6); 68.11(6)	67.9(1); 67.1(1); 69.8(1); 63.8(1) (to nonbonding N)	69.7(1); 65.2(1) (to nonbonding N); 69.4(1); 65.5(1) (to nonbonding N)	66.1(1); 68.7(1); 67.6(1); 66.2(1)	68.0(1); 66.1(1); 66.6(1); 68.7(1)

[a]These long contacts are considered as non-bonded separations.

F2, $^1J_{31P\text{-}109Ag}$ (658 Hz), which is in the same order of magnitude and in contrast to the doubly-bridged cations, where the splitting pattern in F1 was doubled with respect to $^1J_{31P\text{-}109Ag}$. Therefore, we conclude that the minor product of the 2:2:1 mixture of $Ag[PF_6]$, 6,6'-Me_2bpy and dppa in acetone-d_6 at 208 K is the singly-bridged $[Ag_2(dppa)(tpy)_2][PF_6]_2$, which undergoes rapid exchange with the doubly-bridged cation at higher temperature.

Crystal structure of $[Ag_2(dppa)(6,6'\text{-}Me_2bpy)_2][PF_6]_2\cdot Et_2O$

Colourless crystals were grown by layer diffusion of Et_2O into a CH_2Cl_2 solution of $[Ag_2(dppa)(6,6'\text{-}Me_2bpy)_2][PF_6]_2$. The compound crystallizes in the space group $P\bar{1}$ and the asymmetric unit contains one complex cation, two $[PF_6]^-$ anions and one Et_2O molecule. The complex (Fig. 10) consists of two Ag^+ cations which are each chelated by a 6,6'-Me_2bpy

ligand with Ag–N distances between 2.249(2) and 2.302(2) Å and bridged by one dppa molecule, with relatively short Ag–P distances of 2.3475(6) and 2.3390(7) Å.

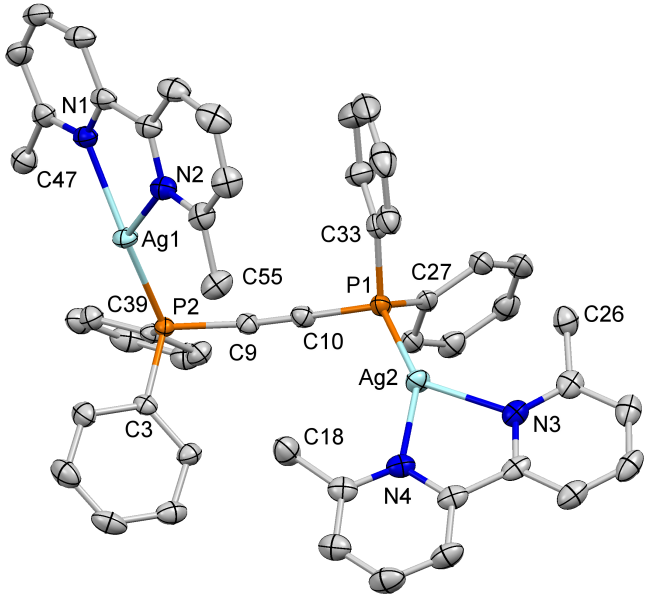

Fig. 10. Structure of $[Ag_2(dppa)(6,6'\text{-}Me_2bpy)_2][PF_6]_2\cdot Et_2O$; H atoms and solvent molecules omitted for clarity. Ellipsoids are plotted at 50% probability level. Selected bond parameters are listed in Table 2.

Each silver centre is coordinated in a trigonal planar geometry, each by two nitrogen atoms and one phosphorus atom (Fig. 10). Atoms N1, N2 and P2 form the trigonal plane around Ag1, with interligand bond angles of P2–Ag1–N1 = 150.29(6)°, P2–Ag1–N2 = 129.72(6)° and N1–Ag1–N2 = 73.25(9)°. The three angles sum up to approximately 353°; the small deviation from 360° fits well with the displacement of the silver cation from the trigonal plane (ca. 0.30 Å). This could be due to Ag1 exhibiting short contacts to F5 (2.912(2) Å) and F6 (2.892(2) Å) of the $[PF_6]^-$ anion (Fig. 11), which is accommodated in a pocket. Taking F5 and F6 into consideration, Ag1 is quasi 5-coordinate. For Ag2, the respective angles are P1–Ag2–N3 = 135.41(7)°, P1–Ag2–N4 = 150.53(7)° and N3–Ag2–N4 = 73.63(9)°, summing to 359.57(13)° and displacing Ag2 almost in the plane of P1, N3 and N4 (distance ca. 0.08 Å). This is in good agreement with the geometry around the Cu^+ cations in $[Cu_2(dppa)(dppf)_2]^{2+}$, where the angles sum up to 360° and the displacement of the Cu^+ cation is 0.02 Å.[21]

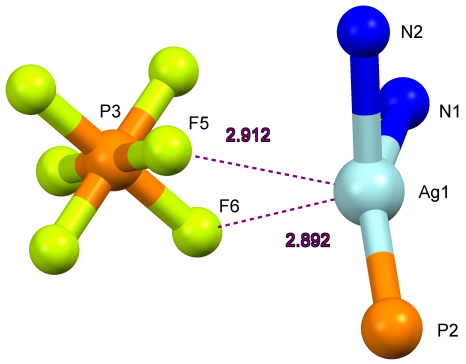

Fig. 11. Coordination geometry around Ag1, showing the coordinated nitrogen atoms of the bipyridine, one phosphorus atom of dppa and the close contacts to F5 and F6 of one $[PF_6]^-$ anion.

Fig. 12 shows a view down the dppa bond and shows an eclipsed conformation. One phenyl group of P2 (containing C39) is on top of the phenyl group of P1 containing C27 and the each of the 6,6'-Me_2bpy ligand lies over a phenyl group of the opposite phosphane. The angles involving the coordinated dppa ligands are Ag1–P2–C9 = 105.74(9)° and Ag2–P1–C10 = 116.15(9)° and the Ag–P–P–Ag torsion angle is found to be 108.14(3)°. Due to the low energy barrier for the rotation of the ethyne bond and phosphorus-C_{ethyne} bonds, a number of different conformers are possible (Scheme 3). Although the pyridine ring with N2 and the phenyl ring containing C33 appear roughly placed on top of each other, the displacement of 24.2° of the ring planes and the centroid-centroid distance of about 4.23 Å make π-π interactions rather inefficient and they can therefore be disregarded as a possible driving force to favour this particular conformer in the solid state.[39] When it comes to solutions, the presence of two conformers in acetone-d_6 was confirmed by NMR spectroscopy (see NMR section). It was not possible to assign the solution species to particular conformers, nor to say whether the dominant solution species agrees with the solid-state structure. Starting with the geometry from the crystal structure, structures of the six conformers on Scheme 3 were optimized at a molecular mechanics (MMFF) level[40] and were found to have very similar energies. This is probably not surprising, given the spatial separation of the Ag atoms and phenyl groups across the P–C≡C–P unit. For the optimizations, the N–Ag–N and N–Ag–P bond angles were constrained to 74 and 143°, respectively, to maintain a trigonal planar geometry at silver.

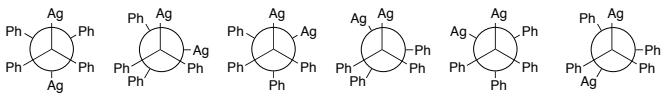

Scheme 3. Newman projections (along the P–C≡C–P vector) showing possible conformers of $[Ag_2(dppa)(6,6'\text{-}Me_2bpy)_2]^{2+}$. Only the positions of the Ag atoms and Ph groups in the gauche and anti-conformers are shown. The second (from left) conformer corresponds to the solid-state structure.

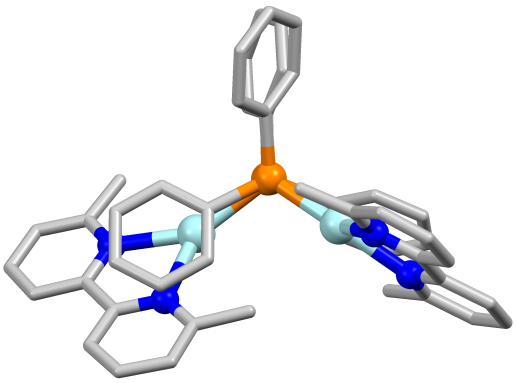

Fig. 12. Looking down the dppa bond from P1 to P2 shows the eclipsed structure with one dppa phenyl group on top of the phenyl group attached to the other phosphorus atom and the bipyridines on top of the respective opposite phenyl ring.

Crystal structure of $[Ag_2(dppa)_2(tpy)_2][PF_6]_2 \cdot 2(CH_3)_2CO$ (pseudo-polymorph 1)

Single crystals of $[Ag_2(dppa)_2(tpy)_2][PF_6]_2 \cdot 2(CH_3)_2CO$ were obtained from a stored NMR tube containing a sample of the compound in acetone-d_6. The compound crystallizes in the triclinic space group $P\bar{1}$. The asymmetric unit contains half a dimer, one $[PF_6]^-$ anion and one acetone molecule per asymmetric unit; the second half of the dimer is symmetry generated by inversion (Fig. 13). All nitrogen atoms of the tpy are attached to the silver cations, with Ag–N distances of 2.3934(17) Å for the middle nitrogen and 2.5100(18) and 2.5179(18) for the outer nitrogen atoms. With C9–C9 distances (or C10–C10 distances, respectively) of 4.113(3) Å, the dppa bridges are relatively close to each other. The dppa bridges are slightly bent inwards (distance P1–P2 = 4.1480(9) Å) and the Ag–P distances of 2.4608(5) and 2.4228(5) Å are slightly longer than in the singly-bridged $[Ag_2(dppa)(6,6'\text{-}Me_2bpy)_2]^{2+}$ cation.

If we focus on the bonds between the outer nitrogen atoms of the tpy ligand and the phosphorus atoms of the two dppa bridges towards the silver cation, the coordination geometry could be described as distorted tetrahedral (as was expected) with the following angles: P_i–Ag1–P2 = 116.286(18)°, P_i–Ag1–N3 = 100.15(5)°, P2–Ag1–N3 = 111.47(5)°, N3–Ag1–N1 = 134.71° and P1–Ag1–N1 = 96.00°. There are no close contacts between cations and anions or solvent molecules and also the packing shows no interactions such as for example stacking.

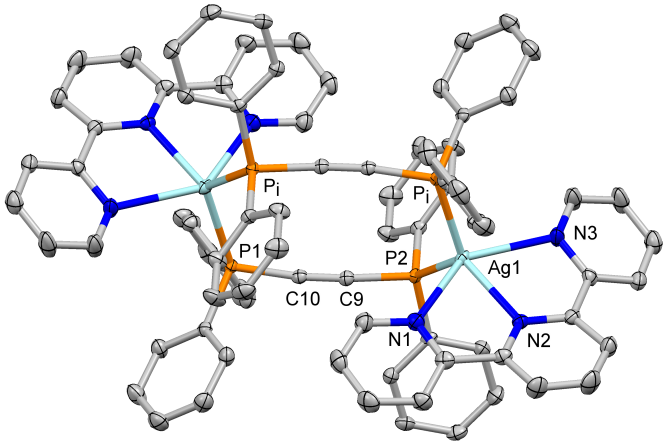

Fig. 13. Structure of $[Ag_2(dppa)_2(tpy)_2][PF_6]_2 \cdot 2Et_2O$; H atoms and solvent molecules omitted for clarity. Ellipsoids are plotted at 50% probability level. Selected bond parameters are listed in Table 2.

Crystal structure of $[Ag_2(dppa)_2(tpy)_2][PF_6]_2 \cdot CH_2Cl_2$ (pseudo-polymorph 2)

Large single crystals of $[Ag_2(dppa)_2(tpy)_2][PF_6]_2 \cdot CH_2Cl_2$ were grown by slow diffusion of Et_2O into a concentrated solution of the compound in CH_2Cl_2. The unit cell is monoclinic $P2_1/c$. In the unit cell, four crystallographically independent $[Ag_2(dppa)_2(tpy)_2]^{2+}$ cations are present (Fig. 14) and show the potential for tpy to act as a hypodentate ligand,[41] with bi-and tridentate coordinated tpy ligands coexisting in the same structure. Figure 14 shows the structures of the four independent dications and Table 2 gives an overview of the important bond parameters, compared to the above discussed structure of $[Ag_2(dppa)_2(tpy)_2][PF_6]_2 \cdot 2Et_2O$ and to $[Ag_2(dppa)(6,6'\text{-}Me_2bpy)_2][PF_6]_2 \cdot Et_2O$. In the dications containing Ag5 and Ag6 or Ag7 and Ag8, all tpy ligands are tridentate. The dimer with Ag1 and Ag2 can be regarded as an intermediate, with one tpy coordinating through all three nitrogen atoms and the other tpy only with two. In the $[Ag_2(dppa)_2(tpy)_2]^{2+}$ cation with Ag3 and Ag4, both tpy ligands are bidentate and each has one non-coordinated nitrogen. While the bonded nitrogen atoms in this pseudo-polymorph have distances between ~ 2.36 and 2.58 Å, the distances that are considered non-bonding are longer (between around 2.73 and 2.76 Å). The same phenomenon of tpy in both a bidentate and tridentate coordination mode in the same crystal structure was found for $[Cu(tpy)(POP)]^+$ where one copper cation is tetra-coordinated and the other penta-coordinated. With Cu–N distances of around 2.1, 2.2 and 2.6 Å for the penta-coordinated cation and ca. 2.1, 2.1 and 3.1 Å for the tetra-coordinated cation, the bond distance between the bonded nitrogen atoms and the copper is significantly longer than for the unattached nitrogen, part a consequence of the third pyridine ring being oriented with the nitrogen facing away from the metal centre.[37]

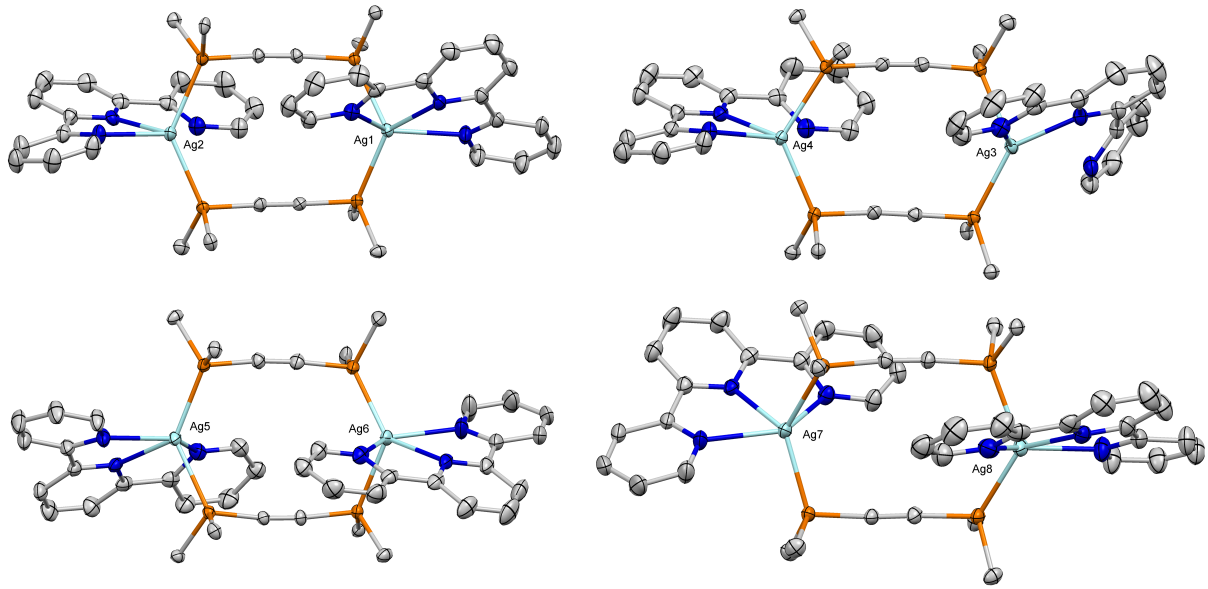

Fig. 14. Structure of $[Ag_2(dppa)_2(tpy)_2][PF_6]_2 \cdot CH_2Cl_2$; H atoms and solvent molecules omitted for clarity. Ellipsoids are plotted at 50% probability level. Selected bond parameters are listed in Table 2.

Conclusions

Four silver complexes containing heteroleptic dications have been synthesized and characterized. Depending on the number of available bisphosphane bridges and the type of chelating nitrogen donor ligand, the coordination modes of the silver cations range from tricoordinate to pentacoordinate and underline the versatility of silver(I) as well as the unpredictability of the outcome of the self-assembly processes. Detailed ^{109}Ag-^{31}P HMQC measurements point out correlations between the number of coordinated phosphorus atoms at the silver and the $^1J_{31P\text{-}109Ag}$ versus the $^1J_{109Ag\text{-}31P}$ coupling constants as well as the chemical shift δ in the ^{109}Ag NMR spectra, which provides a useful tool for the characterization of similar compounds. The crystal structure of the singly-bridged $[Ag_2(dppa)(6,6'\text{-}Me_2bpy)_2]^{2+}$ cation shows an unexpected eclipsed conformation of the 2,2'-bipyridine and the phenyl rings of dppa and finally, a combination of bi- and tridentate for 2,2':6',2"-terpyridine ligands are found in different $[Ag_2(dppa)_2(tpy)_2]^{2+}$ cations and confirm the ability of 2,2':6',2"-terpyridine to exhibit hypodentate coordination.

Acknowledgements

We thank the Swiss National Science Foundation (Grant number 200020_162631) and the University of Basel for support. We are grateful to Thomas Müntener for helpful discussions on the product operator description of AX_2 spin systems and Felix Raps and Nathalia Münch for assistance with low temperature NMR spectra (both University of Basel).

Notes and references

[a]Department of Chemistry, University of Basel, BPR 1096, Mattenstrasse 24a, CH-4058 Basel, Switzerland; email: catherine.housecroft@unibas.ch
[b]Current address: Department of Physics, University of Basel, Klingelbergstrasse 82, CH-4056 Basel, Switzerland
[c]Department of Chemistry, University of Basel, St. Johanns-Ring 19, CH-4056 Basel, Switzerland

†Electronic Supplementary Information (ESI) available: CCDC 1580157-1580159. Figs. S1–S14: Additional NMR spectra. See DOI: 10.1039/b000000x/

1 D. G. Cuttell, S.-M. Kuang, P. E. Fanwick, D. R. McMillin and R. A. Walton, *J. Am. Chem. Soc.*, 2002, **124**, 6.
2 S.-M. Kuang, D. G. Cuttell, D. R. McMillin, P. E. Fanwick and R. A. Walton, *Inorg. Chem.*, 2002, **41**, 3313.
3 R.D. Costa, D. Tordera, E. Ortí, H.J. Bolink, J. Schönle, S. Graber, C.E. Housecroft, E.C. Constable and J.A. Zampese, *J. Mater. Chem.* 2011, **21**, 16108.

4 S. Keller, E. C. Constable, C. E. Housecroft, M. Neuburger, A. Prescimone, G. Longo, A. Pertegás, M. Sessolo and H. J. Bolink, *Dalton Trans.*, 2014, **43**, 16593.

5 S. Keller, A. Pertegás, G. Longo, L. Martinez, J. Cerdá, J.M. Junquera-Hernández, A. Prescimone, E. C. Constable, C. E. Housecroft, E. Ortí and H. J. Bolink, *J. Mater. Chem. C*, 2016, **4**, 3857.

6 R. Czerwieniec and H. Yersin, *Inorg. Chem.*, 2015, **54**, 4322.

7 D. Asil, J. A. Foster, A. Patra, X. de Hatten, J. del Barrio, O. A. Scherman, J.R. Nitschke and R. H. Friend, *Angew. Chem. Int. Ed.*, 2014, **53**, 8388.

8 N. Armaroli, G. Accorsi, M. Holler, O. Moudam, J.-F. Nierengarten, Z. Zhou, R.T. Wegh and R. Welter, *Adv. Mater.*, 2006, **18**, 1313.

9 C. Bizzarri, C. Strabler, J. Prock, B. Trettenbrein, M. Ruggenthaler, C.-H. Yang, F. Polo, A. Iordache, P. Brüggeller and L. De Cola, *Inorg. Chem*., 2014, **53**, 10944.

10 M.D. Weber, C. Garino, G. Volpi, E. Casamassa, M. Milanesio, C. Barolo and R.D. Costa, *Dalton Trans.*, 2016, **45**, 8984.

11 F. Brunner, L. Martínez-Sarti, S. Keller, A. Pertegás, A. Prescimone, E.C. Constable, H.J. Bolink and C.E. Housecroft, *Dalton Trans.*, 2016, **45**, 15180.

12 S. Durini, G. A. Ardizzoia, B. Therrien and S. Brenna, *New J. Chem.* 2017, **41**, 3006.

13 M. Z. Shafikov, A. F. Suleymanova, R. Czerwieniec and H. Yersin, *Chem. Mater.* 2017, **29**, 1708.

14 O. Moudam, A. C. Tsipis, S. Kommanaboyina, P. N. Horton and S. J. Coles, *RSC Adv.* 2015, **5**, 95047.

15 O. Moudam, N. Bristow, S.-W. Chang, M. Horieb and J. Kettle, *RSC Adv.* 2015, **5**, 12397.

16 W. Weymiens, J. C. Slootweg and K. Lammertsma, in *Phosphorus Compounds. Advanced Tools in Catalysis and Material Sciences*, ed. M. Peruzzini and L. Gonsalvi, Springer International Publishing AG, Dordrecht, Netherlands, Vol. 37, 1st edn, 2011, pp. 21–55.

17 A. K. Powell and M. J. Went, *J. Chem. Soc. Dalton Trans.*, 1992, 439.

18 M. Haehnel, S. Hansen, K. Schubert, P. Arndt, A. Spannenberg, H. Jiao and U. Rosenthal, *J. Am. Chem. Soc.*, 2013, **135**, 17556.

19 A. Fazal, B. El Ali, L. Ouahab and M. Fettouhi, *Polyhedron*, 2013, **49**, 7.

20 A. Fazal, A. Al-Dawsari, B. El Ali, L. Ouahab and M. Fettouhi, *Journal of Coordination Chemistry*, 2014, **67**, 14, 2357.

21 Y.-C. Liu, C.-I. Li, W.-Y. Yeh, G.-H. Lee and S.-M. Peng, *Inorganica Chimica Acta,* 2006, **359**, 2361.

22 H.-W. Xu, L.-X. Zhang, Y.-H. Li and H.-F. Wang, *Synth. React. Inorg., Met.-Org., Nano-Met. Chem.*, 2011, **41**, 743.

23 A. Kaeser, B. Delavaux-Nicot, C. Duhayon, Y. Coppel and J.-F. Nierengarten, *Inorg. Chem.*, 2013, **52**, 14343.

24 E. Lozano, M. Nieuwenhuyzen and S. L. James, *Chem. Eur. J.*, 2001, **7**, 12, 2644.

25 M.-C. Brandys and R. J. Puddephatt, *J. Am. Chem. Soc.*, 2002, **124**, 3946.

26 S. L. James, E. Lozano and M. Nieuwenhuyzen, *Chem. Commun.*, 2000, 617.

27 G. H. Penner and X. Liu, *Prog. Nucl. Magn. Reson. Spectrosc.*, 2006, **49**, 151.

28 S. J. Berners-Price, R. J. Bowen, P. J. Harvey, P. C. Healy and G. A. Koutsantonis, *J. Chem. Soc., Dalton Trans.* 1998, 1743.

29 F. Lianza, A. Macchioni, P. Pregosin and H. Ruegger, *Inorg. Chem.* 1994, **33**, 4999.

30 C.-W. Burges, R. Koschmieder, W. Sahm, and A. Schwenk, *Z. Naturforsch.,* 1973, **28a**, 1753.

31 D. L. Jameson and L. E. Guise, *Tetrahedron Lett.*, 1991, **32**, 1999.

32 Bruker Analytical X-ray Systems, Inc., 2006, APEX2, version 2 User Manual, M86-E01078, Madison, WI.

33 P. W. Betteridge, J. R. Carruthers, R. I. Cooper, K. Prout and D. J. Watkin, *J. Appl. Cryst*., 2003, **36**, 1487.

34 I. J. Bruno, J. C. Cole, P. R. Edgington, M. K. Kessler, C. F. Macrae, P. McCabe, J. Pearson and R. Taylor, *Acta Crystallogr., Sect. B*, 2002, **58**, 389.

35 C. F. Macrae, I. J. Bruno, J. A. Chisholm, P. R. Edgington, P. McCabe, E. Pidcock, L. Rodriguez-Monge, R. Taylor, J. van de Streek and P. A. Wood, *J. Appl. Cryst*., 2008, **41**, 466.

36 POMA, v. 2.0; P. Güntert, N. Schaefer, G. Otting and K. Wüthrich, *J. Magn. Reson. A*, 1993, **101**, 103.

37 N. S. Murray, S. Keller, E. C. Constable, C. E. Housecroft, M. Neuburger and A. Prescimone, *Dalton Trans*., 2015, **44**, 7626.

38 S.M. Socol and J.G. Verkade, *Inorg. Chem.*, 1984, **23**, 3487.

39 C. Janiak, *J. Chem. Soc., Dalton Trans.*, 2000, 3885.

40 Spartan '16, v. 2.0.5, Wavefunction Inc.

41 E. C. Constable and C. E. Housecroft, *Coord. Chem. Rev.*, 2017, **350**, 84.